Characterization of Some Polyacrylonitrile-Based Electrolytes

H. S. Choe, B. G. Carroll, D. M. Pasquariello, and K. M. Abraham*

EIC Laboratories, Inc., 111 Downey Street, Norwood, Massachusetts 02062

Received July 31, 1996. Revised Manuscript Received September 13, 1996[⊗]

Polyacrylonitrile (PAN)-based electrolytes have been prepared by encapsulating Li salt solutions obtained by dissolving $LiN(SO_2CF_3)_2$, $LiAsF_6$, $LiSO_3CF_3$, or $LiPF_6$ in a plasticizer mixture of ethylene carbonate (EC) and propylene carbonate (PC). The conductivity of these electrolytes is governed by a combination of factors including the relative amounts of PAN, EC, PC and the Li salt, and temperature. A conductivity of about $4.5 \times 10^{-3}\ \Omega^{-1}\ cm^{-1}$ at 30 °C was exhibited by EC-rich electrolytes containing both $LiN(SO_2CF_3)_2$ and $LiPF_6$. The cationic transference numbers, measured using a dc polarization method coupled with impedance spectroscopy, were found to be between 0.2 and 0.3 for electrolytes containing $LiN(CF_3SO_2)_2$ and $LiPF_6$. The tensile strength of the electrolytes was observed to increase from 60 to 140 lb/in.^{2} upon incorporation of the thermally activated cross-linking agent ethylene glycol dimethacrylate. Cyclic voltammetry on Pt electrodes has shown that these electrolytes have an inherent oxidation stability window extending up to about 5 V versus Li^+/Li. On Al, Ni, and Cu electrodes, however, oxidation was observed at lower potentials because of metal corrosion reactions. Copper was reversibly oxidized at 3.5 V, irrespective of the Li salt present in the electrolyte. On the other hand, the nature of the Li salt influenced the corrosion potentials of Al and Ni. Nickel was found to be stable up to 4.2 V in the presence of $LiAsF_6$, whereas it was oxidized at about 3.5 and 4 V when the electrolyte contained $LiN(SO_2CF_3)_2$ and $LiSO_3CF_3$, respectively. Aluminum electrodes showed no oxidation currents up to 4.2 V when the salts were $LiPF_6$ and $LiAsF_6$ which contrasted the behavior with $LiN(SO_2CF_3)_2$ and $LiSO_3CF_3$ showing oxidation at $\leq$4 V. The electrochemical stability of the electrolytes was further verified in $Li/LiMn_2O_4$ cells.

Introduction

The increasing interest in all-solid-state, high-energy-density, rechargeable Li and Li-ion batteries is a strong driving force for the development of solid polymer electrolytes (SPE) with high room-temperature conductivities. To be able to compete with liquid-electrolyte-based batteries, which typically can be discharged at current densities of several mA/cm^2 (i.e., C/10 to C rates), solid polymer electrolytes must exhibit conductivities of the order of $10^{-3}\ \Omega^{-1}\ cm^{-1}$ at room temperature. These electrolytes should also possess a wide electrochemical stability window, preferably between 0 and 4.5 V vs Li^+/Li, to be compatible with high-voltage cathodes such as TiS_2, V_6O_{13}, $LiMn_2O_4$, $LiNiO_2$, and $LiCoO_2$ and low-voltage anodes such as Li and Li_xC_6. Finally, the polymer electrolytes should possess good dimensional stability so that they can be processed into free-standing thin films suitable for serving as separators in the battery.

Recently, we have reported[1−3] on the preparation of a series of Li^+ conductive electrolytes based on polyacrylonitrile (PAN) with room-temperature conductivities of about $2 \times 10^{-3}\ \Omega^{-1}\ cm^{-1}$. These electrolytes, comprising solutions of Li salts in a mixture of ethylene carbonate (EC) and propylene carbonate (PC) immobilized in PAN, have been isolated as free-standing thin films, and their suitability for the development of solid-state Li and Li-ion batteries has been demonstrated.[1]

In this paper we present a detailed account of the conductivity and electrochemical oxidation stability of a group of PAN-based electrolytes. The conductivity over the temperature of −10 to 50 °C was investigated as a function of the nature of the Li salt and the EC:PC ratio in the electrolyte, thereby identifying electrolyte compositions having the highest ambient temperature conductivity. The transference numbers of the various PAN-based electrolytes were measured to determine the relative contributions of the cation and anions to ionic conduction. The electrochemical oxidation stabilities of the electrolytes were examined on a variety of electrodes including carbon (C), aluminum (Al), nickel (Ni), copper (Cu), stainless steel (SS), and platinum (Pt), and the influence of Li salts on the stability of the electrolytes was studied. In an attempt to improve the mechanical strength, the PAN-based polymer electrolyte was modified with ethylene glycol dimethacrylate (EGD) and vinyl sulfone (VS) which formed interpenetrating networks.

Experimental Procedure

Electrolyte preparation and electrochemical measurements were conducted in a Vacuum Atmospheres Corp. (Hawthorne, CA) glovebox purged with argon.

* Author to whom correspondence should be addressed.

[⊗] Abstract published in *Advance ACS Abstracts,* November 1, 1996.

(1) Abraham, K. M.; Alamgir, M. *J. Electrochem. Soc.* **1990**, *136*, 1657.

(2) Alamgir, M.; Abraham, K. M. In *Lithium Batteries, New Materials, Developments and Perspectives*; Pistoia, G., Ed.; Elsevier: New York, 1994; Chapter 3.

(3) Abraham, K. M.; Alamgir, M. *J. Power Sources* **1993**, *43−44*, 195.

S0897-4756(96)00412-7 CCC: $14.00

Polyacrylonitrile (PAN, Polysciences, Warrington, PA, MW = 100 000) was dried under vacuum at 40 °C for 24 h. Propylene carbonate (Scientific Products, IL), and ethylene carbonate (Baxter, IL), were purified by distilling under vacuum. Vinyl sulfone (VS, Aldrich, WI) was purified by passing it through an ion-exchange column. $LiN(CF_3SO_2)_2$ (3M, Minneapolis, MN) was dried at 140 °C under vacuum for 24 h. $LiCF_3SO_3$, (3M, Minneapolis, MN) was dried at 100 °C under vacuum for 24 h. $LiPF_6$ (Advance Research Chemicals, OK), $LiAsF_6$ (FMC, NC), and ethylene glycol dimethacrylate (Aldrich, WI) were used as-received.

Electrolyte Preparation. The PAN-based electrolytes were prepared as follows. The Li salt (LiX where X = $CF_3SO_3^-$, $N(CF_3SO_2)_2^-$, PF_6^-, or AsF_6^-) was first dissolved in an EC/PC solvent mixture with the desired EC to PC ratio. A known amount of PAN, as required by the electrolyte composition, was then added to the salt solution, and the entire mixture was heated in a closed vial at about 135 °C, until the polymer dissolved and formed a homogeneous solution. The viscous solution was then placed between two metal sheets covered with Teflon release films and rolled between two rollers to obtain a thin film. Mechanically strong polymer electrolyte films of thicknesses ranging between 50 and 80 μm were obtained.

Conductivity. The conductivities of PAN-based electrolytes were measured by means of impedance spectroscopy. The test cell consisted of the solid electrolyte film sandwiched between two stainless steel (SS) blocking electrodes, which were spring-loaded to provide good contact between the electrolyte and the electrodes. The entire setup was housed in a tightly sealed glass jar, and the conductivities were measured over the temperature range of −10 to 50 °C. The EG&G PAR Model 273 potentiostat/galvanostat in conjunction with a PAR Model 5208 lock-in amplifier was used for measuring the impedance spectra. In a typical measurement, a 10 mV ac signal was applied to the conductivity cell, and its impedance was measured in the frequency range from 5 Hz to 100 kHz. The electrolyte resistance was determined from the Cole−Cole plots of the resulting impedance data. The plot of the imaginary part of the impedance versus the real part consisted of a slanted spike displaced from the origin, representative of a resistor in series with a capacitor. The resistance was measured from the high frequency intercept on the real axis. The electrolyte conductivity was calculated from the measured resistance and the known thickness and area of the film.

Transference Number Measurements. The transference numbers were measured using a technique that combines both the dc and ac polarization methods, first described by Evans et al.[4] The electrochemical cell comprised a rectangular piece of polymer electrolyte (about 4 cm^2) sandwiched between two nonblocking electrodes made of lithium foil (about 1.7 cm^2). The impedance of the cell was measured using EG&G PAR (Model 273) potentiostat/galvanostat and EG&G lock-in analyzer (Model 5208) between the frequencies of 0.1 Hz and 100 kHz, before and after applying a constant potential difference across the electrodes. Direct current polarization was carried out by applying a potential, ranging between 7 and 100 mV, to the symmetrical cell using an EG&G PAR (Model 273) potentiostat/galvanostat. The resulting current was measured as a function of time. All the measurements were conducted in an argon-filled dry-box at room temperature.

Mechanical Strength. PAN-based polymer electrolyte was modified by adding small amounts (about 4 w/o) of monomers such as VS and EGD to the polymer electrolyte mixture which formed interpenetrating networks during the thermal processing of the films. Benzoyl peroxide was used as the thermal initiator. The relative strength of the baseline and the modified SPEs were measured using an Instron tensile tester equipped with a 100 lb load cell and interfaced to an IBM-compatible computer for data collection. The SPE samples having the dimensions of 1 in. × 6 were pulled at a constant rate of 2 in./min.

(4) Evans, J.; Vincent, C. A.; Bruce, P. G. *Polymer* **1987**, *28*, 2324.

Electrochemical Stability. Electrochemical stabilities of the electrolytes were evaluated from cyclic voltammetric experiments, using an EG&G PAR (Model 273) potentiostat/galvanostat. A three-electrode electrochemical cell, comprising a working electrode, a lithium counter electrode, and a lithium reference electrode, was used. Working electrodes of Ni, Al, SS, Cu, Pt, and carbon were used to study the effect of the electrode material on electrochemical stability. The measurements were conducted in an argon-filled drybox at room temperature. The electrodes were scanned at a rate of 1 mV/s, and all potentials are recorded with respect to Li^+/Li.

Li/SPE/$LiMn_2O_4$ Cell. Li/SPE/$LiMn_2O_4$ cell was fabricated as described in ref 3, where the composite cathode comprised a mixture of spinel $LiMn_2O_4$, polymer electrolyte binder, and acetylene black in the ratio of 50:42.2:7.8. The SPE comprised PAN/EC−PC/$LiAsF_6$. The cell was enclosed in a metallized plastic bag, which was evacuated and sealed at the edges. The electrochemical performance of the cells were carried out using an Arbin battery test system (Bryan, TX).

Results and Discussion

Conductivities of PAN-Based Electrolytes. The PAN-based electrolytes, composed of PAN, EC, PC, and a Li salt, were isolated as free-standing thin films with thickness ranging from 50 to 80 μm. They are transparent materials with a water-clear appearance. Polyacrylonitrile is a linear polymer (I), while EC (II) and PC (III) are low volatility organic carbonate solvents.

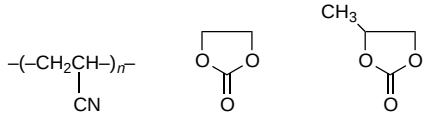

I II III

All of the electrolytes were first characterized in terms of their conductivities. The conductivity (σ) was calculated from the resistance (R) of the electrolyte film using the equation,

$$\sigma = l/RA \qquad (1)$$

where l is the thickness of the electrolyte film (in cm) and A is its area (in cm^2).

The conductivities measured over the temperature range of −10 to 50 °C were analyzed to determine how the nature of the Li salt and the relative amounts of EC and PC in the electrolytes affected conductivity. The salts studied were $LiAsF_6$, $LiCF_3SO_3$, $LiN(SO_2CF_3)_2$, and $LiPF_6$. It was found that the solubility of a salt depended on the amounts of PC and EC in the film, while the ability to prepare a free-standing film depended on the amount of PAN present. However, as shown in Table 1, the amount of PAN required to form a free-standing electrolyte film did not vary significantly from one salt to the other. Table 1 gives a list of the electrolytes investigated along with their conductivities measured at 30 °C. Specific conductivities in the range $(4.0-4.7) \times 10^{-3}$ Ω^{-1} cm^{-1} were exhibited by several electrolytes containing $LiN(SO_2CF_3)_2$ and $LiPF_6$. The temperature dependence of conductivities plotted in the Arrhenius fashion are presented in Figures 1−3. The low activation energies calculated from these plots, and listed in Table 1, are consistent with an ionic transport that is assisted more by the solvent than by the segmental motion of the polymer chains.

The data in Figure 1 for electrolytes containing $LiN(SO_2CF_3)_2$ indicate a strong influence of the relative

Table 1. Compositions (in weight percent (w/o)) and Conductivities of Some PAN-Based Electrolytes

electrolyte no.	PAN (w/o)	EC (w/o)	PC (w/o)	Li Salt (w/o)	$\sigma_{30°C}$ (10^{-3} Ω^{-1} cm^{-1})	E_a[a] (kcal/mol)
1	16.0	40.0	40.0	4.0/$LiCF_3SO_3$	1.00	4.5
2	13.0	61.7	15.4	10.0/$LiCF_3SO_3$	1.7	
3	14.2	39.3	39.3	7.1/$LiN(CF_3SO_2)_2$	2.11	3.3
4	12.8	57.1	14.3	15.8/$LiN(CF_3SO_2)_2$	4.30	4.3
5	12.8	71.4	0	15.8/$LiN(CF_3SO_2)_2$	4.62	4.1
6	13.5	37.5	37.5	11.6/$LiAsF_6$	1.99	4.8
7	13.0	75.0	0	12.0/$LiAsF_6$	3.61	4.6
8	14.0	39.0	39.0	8.0/$LiPF_6$	2.36	4.2
9	13.9	61.7	15.4	9.1/$LiPF_6$	3.73	4.7
10	17.0	74.0	0	9.0/$LiPF_6$	1.97	4.9
11	13.0	77.5	0	9.5/$LiPF_6$	4.67	3.7
12	13.0	61.6	15.4	10.0/$LiPF_6$	2.75	4.6
13	12.0	59.2	14.8	14.0/$LiPF_6$	4.01	5.2
14	12.0	37.0	37.0	14.0/$LiPF_6$	3.83	4.3

[a] Calculated from conductivity data in the −10 to 50 °C range using the Arrhenius equation, $\sigma = \sigma_0 e^{-E_a/RT}$.

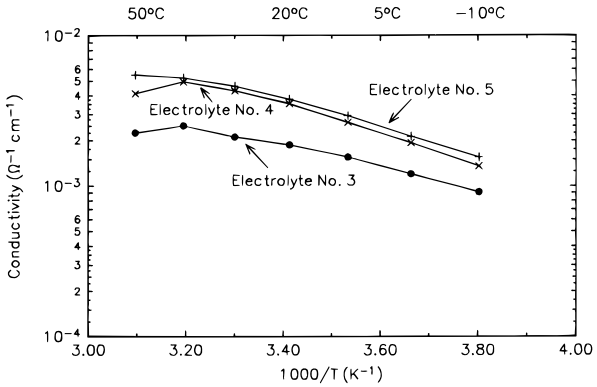

Figure 1. Conductivities of electrolytes containing $LiN(CF_3SO_2)_2$.

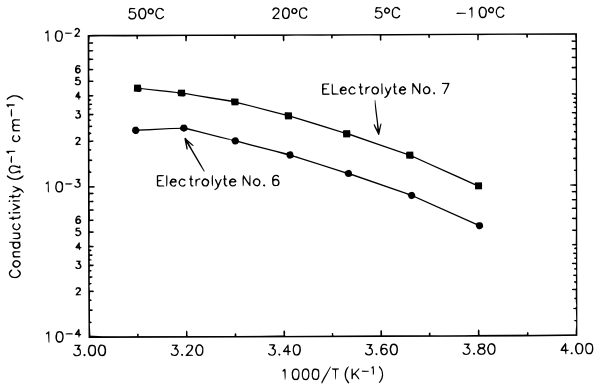

Figure 2. Conductivities of electrolytes containing $LiAsF_6$.

amounts of EC and PC on conductivity. Electrolyte no. 5 containing only EC as the plasticizer has the highest overall conductivity in this group at room temperature. Generally higher conductivities were observed at temperatures between −10 and 50 °C when the plasticizer mixture was rich in EC. Because of the difficulty in preparing free-standing electrolyte films without any EC, the effect of using only PC as the plasticizer on conductivity could not be assessed.

Behavior similar to that shown by $LiN(SO_2CF_3)_2$-containing electrolytes was found in electrolytes with $LiAsF_6$ and $LiPF_6$. Figure 2 gives a comparison of the conductivities of electrolytes containing $LiAsF_6$ with different amounts of EC and PC. The higher conductivities in the −10 to 50 °C range shown by electrolyte

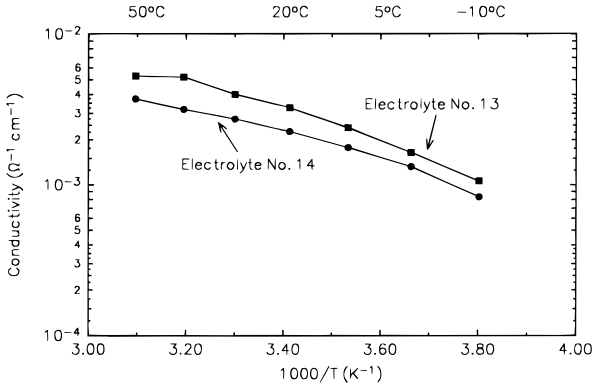

Figure 3. Conductivities of electrolytes containing $LiPF_6$.

no. 7 with only EC as the plasticizing solvent reinforce the observation with electrolytes containing $LiN(SO_2CF_3)_2$ that the greater the amount of EC in the solvent mixture, the greater is the conductivity in the vicinity of room temperature. The results reported in Figure 3 show that the temperature dependence of the conductivities of $LiPF_6$-containing electrolytes follows the same pattern as those containing the other two salts.

The conductivity of an electrolyte can be approximately described by

$$\sigma = \sum z_i n_i \mu_i \qquad (2)$$

where z_i is the ionic charge, n_i is the number of ionic charge carriers, and μ_i is the mobility of the ions.[5] A satisfactory explanation for the observed influence of solvents on conductivity can be given from a knowledge of their melting points, viscosities, and dielectric constants and the molecular structure of the electrolyte. EC is a solid at room temperature with a melting point of 39 °C, while the melting point of PC is −49 °C. EC has a lower viscosity than PC, 1.91 cP vs 2.53 cP at 40 °C, and the dielectric constants of EC and PC are 89.6 and 64.4, respectively. With respect to the structure of the electrolyte, it is recognized[6,7] that the Li ion in a nonaqueous electrolyte is fully solvated by the solvent molecules. The typical coordination number of Li^+ is four, meaning that each Li^+ is solvated by four solvent molecules. In PAN-based electrolytes, interactions of the Li^+ with the C≡N group on polyacrylonitrile has also been recognized.[8]

In electrolytes with high concentrations of Li salts, such as those being discussed here (>1 M), the charge carriers are aggregated ions such as triplets (vide infra), whose abundance is largely determined by the dielectric constants (ϵ) of the plasticizers. Since EC has a significantly higher dielectric constant than PC, it is reasonable to assume higher concentrations of charge carriers in EC-rich electrolytes. EC is also less viscous than PC. Therefore, the higher conductivities of EC-rich electrolytes can be attributed to the existence of a larger number of charge carriers having greater mobility provided by the less viscous EC. It should be noted that

(5) Gray, F. M. *Solid Polymer Electrolytes*; VCH Publishers: New York, 1991.
(6) Blomgren, G. E. In *Lithium Batteries*; Gabano, J. P., Ed.; Academic Press: New York, 1983; Chapter 2.
(7) Abraham, K. M.; Alamgir, M. In *Proceedings of the Science of Advanced Batteries*; Case Western Reserve University, 1993.
(8) Croce, P.; Brown, S. B.; Greenbaum, S. G.; Slane, S. M.; Salomon, M. *Chem. Mater.* **1993**, *5*, 1268.

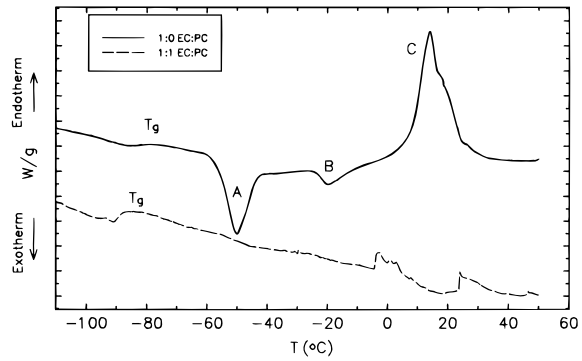

Figure 4. DSC curves for electrolytes containing 1:1 and 1:0 by weight of EC:PC plasticizer mixture.

even in an EC-rich electrolyte, the conductivity decreases significantly when there is a large increase in the PAN content (compare electrolytes 10 and 11). Consequently, factors other than those discussed above are also contributing to the conductivity of these electrolytes.

At temperatures below −10 °C, we find that an EC-poor plasticizer mixture provides higher conductivities. To understand this behavior, differential scanning calorimetry (DSC) measurements were carried out on electrolytes containing different amounts of EC and PC, i.e., 1:0 and 1:1 by weight of EC:PC, at temperatures ranging from −120 to 50 °C. The DSC curves are shown in Figure 4. The electrolyte containing 1:1 by weight of EC:PC exhibits a glass transition temperature, T_g, of −89 °C, which is in agreement with the data obtained by Croce et al.,[9] while the EC-only electrolyte shows a slightly higher T_g of −84 °C. The EC-only electrolyte also exhibits two exotherms at −50 (A) and −20 (B) °C, and an endotherm at around 14 °C (C). The two exotherms could be attributed to the crystallization of two different solvates of Li salt and the endotherm to the melting of the solvate and/or free EC. Since the melting point of EC is 39 °C, the more likely species responsible for the 14 °C endotherm is the solvate. However, the existence of free EC is possible since an examination of the electrolyte compositions given in Table 1 reveals that the molar ratio of the solvent to Li^+ is between 10 and 15, implying that, in addition to the solvates, there is a significant amount of unsolvated (or free) solvent present in each electrolyte. Interestingly, neither exotherms nor endotherms were observed for the electrolyte with equal amounts of EC and PC, indicating that crystallization of both the solvates and EC is suppressed with the addition of PC. Increased ionic mobility in the absence of crystalline species would explain why electrolytes with the EC-poor plasticizer mixtures exhibit higher conductivities at temperatures below −10 °C.

The effect of Li salt concentration on conductivity was studied with the electrolytes listed in Table 2 containing $LiPF_6$. Figure 5 gives a plot of their conductivities as a function of $LiPF_6$ concentrations at different temperatures. The conductivity increases with increasing salt concentration until it reaches a maximum at about 1.4 M $LiPF_6$. With more $LiPF_6$, the conductivities decrease, most likely due to the overriding influence of viscosity

(9) Behl, W. K. *J. Electrochem. Soc.* **1981**, *128*, 939.
(10) Eisenberg, M.; Wong, K. In *Proc. 234d Power Sources Conf.*, Atlantic City, NJ; PSC Publications: Redbank, NJ, 1969.

Table 2. Compositions (in w/o) of Electrolytes Containing 10−14 wt % $LiPF_6$

electrolyte no.	PAN (w/o)	EC (w/o)	PC (w/o)	$LiPF_6$ (w/o)/ (molarity)[a]
16	13.0	61.6	15.4	10.0/(0.93 M)
17	13.0	60.8	15.2	11.0/(1.04 M)
18	13.0	60.0	15.0	12.0/(1.14 M)
19	13.0	59.2	14.8	13.0/(1.25 M)
20	13.0	58.4	14.6	14.0/(1.36 M)

[a] The molarity was calculated on the basis of the number of moles of Li salt per liter of the solution of the salt in the plasticizer solvent.

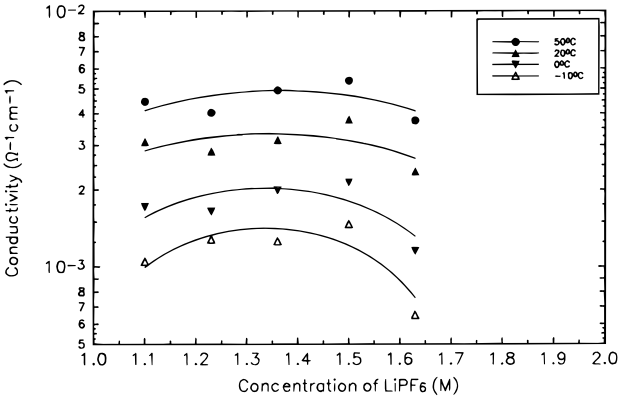

Figure 5. Conductivities of electrolytes containing 13 wt % PAN as a function of various concentrations of $LiPF_6$. The EC:PC ratio in the electrolyte is 4:1 by weight.

Table 3. Relative Viscosity of Solutions Containing Different Amounts of $LiPF_6$ Dissolved in 4:1 by Weight of EC:PC Solvent Mixture

concn of $LiPF_6$ (M)	relative viscosity (η_r)	concn of $LiPF_6$ (M)	relative viscosity (η_r)
1.11	2.85	1.5	4.41
1.23	3.22	1.63	5.07
1.36	3.77		

on ionic mobility. Note that ionic mobility in an electrolyte will decrease as the viscosity of the ionic environment increases.[5] Viscosity measurements were carried out on solutions containing different amounts of $LiPF_6$ dissolved in 4:1 by weight of EC:PC, where the concentration of the salt corresponded to those listed in Table 2. The EC/PC mixture without any salt was used as the standard. Table 3 lists the relative viscosity, $\eta_r = \eta/\eta_0 \approx t/t_0$, where t is the time required for a specified volume of solution to flow through a capillary tube and t_0 is that for the standard. There is a steady increase in the viscosity of the solution as the salt concentration increases, in agreement with the proposal that the conductivity maxima arises from the overriding influence of viscosity.

In summary, the conductivities of PAN-based electrolytes depend on the concentration of the salt and the relative amounts of PAN and the two plasticizing solvents. The highest conductivity of about 4.7×10^{-3} Ω^{-1} cm^{-1} at 30 °C was exhibited by electrolyte no. 11 composed of 13 wt % PAN, 77.5 wt % EC, and 9.5 wt % $LiPF_6$. The two electrolytes containing $LiN(SO_2CF_3)_2$, nos. 4 and 5, have conductivities very close to this value.

Transference Number Measurements. As mentioned earlier, the conductivity of an electrolyte depends on the number and mobility of ionic carriers. When a salt MA is dissolved in a polymer host, a series of equilibria are likely to exist in which associated species

are formed:

$$M^+ + A^- \leftrightarrow MA$$

$$M^+ + MA \leftrightarrow M_2A^+$$

$$A^- + MA \leftrightarrow MA_2^-$$

When an electric field is applied to the polymer electrolyte, the cation constituent M is carried toward the cathode by M^+, M_2A^+, M_3A^{2+}, etc., while A^-, MA_2^-, etc., migrate toward the anode. Hence, the movement of both the cationic and anionic species contribute to the total ionic conductivity. The contribution of the cationic and anionic species to the overall conductivity of the polymer electrolytes can be evaluated by measuring the transference number, T_+, which is defined as the net number of faradays of charge carried across the reference plane by the cationic species in the direction of the cathode, during the passage of one faraday of charge across the plane. The quantity that can be measured experimentally is the difference between the fluxes of M-containing species directed toward the cathode and anode, i.e., the net number of moles of M being transferred in one direction. Hence, the transference number of the cation constituent, T_M, may be related to the individual transference numbers by

$$T_M = t_{M^+} + 2t_{M_2A^+} - t_{MA_2^-}$$

During the application of the electric field, the current is observed to fall with time and a steady state is achieved eventually. This fall in current is considered to result from two processes: (a) the growth at the electrodes of passivating layers, which occurs whether or not a current is flowing, and (b) the establishment of a concentration gradient in the electrolyte which affects the motion of the ions.

Evans et al.[4] have shown that for small amounts of polarization, the initial (I°) and steady-state (I^s) currents are given respectively by

$$I^\circ = \frac{\Delta V}{(R_1^\circ + R_b)} = \frac{\Delta V}{(R_1^\circ + k/\sigma)} \quad (3)$$

$$I^s = \frac{\Delta V}{R_1^s + \frac{k}{T_+\sigma}} \quad (4)$$

where ΔV is the potential applied across the cell, k is the cell constant, T_+ is the cationic transference number, σ is the (dc) conductivity of the electrolyte, R_b is the electrolyte resistance, R_1° and R_1^s are the initial and steady-state resistances of the passivating layers. R_b, R_1°, and R_1^s were obtained by measuring the initial and final impedances of the cell. From eq 3

$$\sigma = \frac{I^\circ k}{(\Delta V - I^\circ R_1^\circ)} \quad (5)$$

and from eqs 4 and 5

$$T_+ = \frac{I^s(\Delta V - I^\circ R_1^\circ)}{I^\circ(\Delta V - I^s R_1^s)} \quad (6)$$

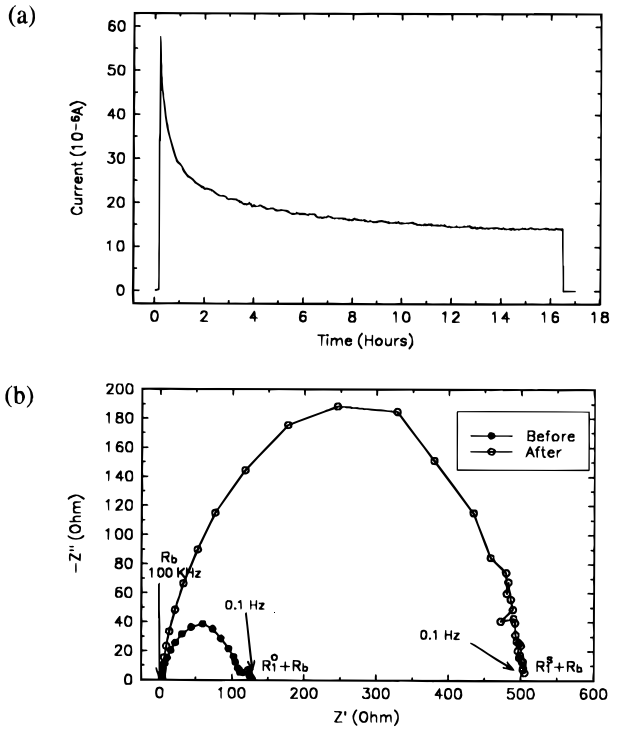

Figure 6. Current−time profile (a) and impedance plots (b) of a symmetrical cell comprising electrolyte no. 1. The dc bias was 7.4 mV.

Table 4. Compositions (in w/o) of Electrolytes Used for Transference Number Measurements

electrolyte no.	PAN (w/o)	EC (w/o)	PC (w/o)	salt (w/o)	RT conductivity (10^{-3} Ω^{-1} cm^{-1})
1	13.5	37.5	37.5	11.6 ($LiAsF_6$)	1.61
2	12.8	71.4	0	15.8($LiN(CF_3SO_2)_2$	3.78
3	14.0	38.5	38.5	9.0 ($LiPF_6$)	2.27

The transference numbers of three different PAN-based polymer electrolytes, whose compositions and room-temperature conductivities are listed in Table 4, were measured.

Figure 6a represents the current vs time plot for electrolyte no. 1, containing $LiAsF_6$, during the application of a dc bias of 7.4 mV across the cell. The initial and final impedance plots are given in Figure 6b. The high-frequency end of the arc (left-hand side) represents the impedance of the bulk electrolyte (R_b), while the low-frequency end (right-hand side) represents the total impedance of the cell ($R_b + R_1^\circ$ or $R_b + R_1^s$), that includes the resistive layer on the electrodes (R_1° and R_1^s). It is apparent that the passivation layer is present even before applying the dc bias since $R_1^\circ = 125.3\ \Omega$, and continues to grow during polarization with $R_1^s = 501.7\ \Omega$. Due to the highly conductive electrolyte, where $R_b = 3.2\ \Omega$, the passivation layer is observed to represent the bulk of the cell impedance. Using eq 3, an initial current of 5.76×10^{-5} A was calculated, and a steady-state current of 1.42×10^{-5} A was obtained from the current−time curve. The cationic transference number was calculated to be $T_+ = 0.16$ using eq 6.

A slightly higher transference number of $T_+ = 0.30$ was obtained for electrolyte no. 2 comprising $LiN(CF_3SO_2)_2$. The resistance of the passivation layers did not increase significantly during polarization, where $R_1^\circ = 90.3\ \Omega$ and $R_1^s = 104.3\ \Omega$, and $I^\circ = 7.96 \times 10^{-5}$ and $I^s = 6.67 \times 10^{-5}$ A. For electrolyte no. 3 containing $LiPF_6$, a very resistive passivation layer ($R_1^\circ = 354\ \Omega$) was

Table 5. Summary of Transference Number Measurements Obtained with a dc Bias of 7.5 mV

electrolyte no.	expt	$R_1°$ (Ω)	R_1^s (Ω)	$I°$ ($\times 10^{-5}$ A)	I^s ($\times 10^{-5}$ A)	V (mV)	T_+
1	a	125.3	501.7	5.76	1.42	7.4	0.16
	b	158.9	430.3	4.55	1.61	7.4	0.13
	c	259.1	1203.7	2.86	0.55	7.5	0.02
	d	144.6	424.9	4.96	1.60	7.4	0.12
2	a	90.3	104.3	7.96	6.67	7.4	0.30
	b	75.7	128.4	10.4	5.73	8.2	0.20
	c	77.7	167.9	8.88	3.90	7.1	0.16
	d	56.6	95.5	12.7	7.2	7.4	0.25
3	a	364	1073	2.04	0.54	7.5	0.01
	b	498.4	915	1.49	0.66	7.5	0.02
	c	811.6	2175.1	0.92	0.29	7.5	0.01

present on the lithium electrodes even before the application of a potential bias. This was observed to increase to about $R_1^s = 1100$ Ω after the application of 7.5 mV across the cell for about 16 h. As a result the initial and final currents were very small, where $I° = 2.04 \times 10^{-5}$ and $I^s = 0.54 \times 10^{-5}$ A. The transference number was calculated to be only 0.01, implying almost no cationic transport in this system.

Several cationic transference number measurements were taken for each electrolyte, and the results are summarized in Table 5. For the electrolyte containing $LiN(CF_3SO_2)_2$ (electrolyte no. 2), T_+ ranged between 0.16 and 0.30. For the electrolyte containing $LiAsF_6$ (electrolyte no. 1), the T_+ values ranged between 0.12 and 0.16, except for electrolyte no. 1(c) where $T_+ = 0.02$. On comparing the resistance of the passivation layer, it is observed that R_1^s for electrolyte no. 1c is about 3 times greater than that of the others in this group (see 1a, b, and d of Table 5). Similar results were obtained with electrolytes containing $LiPF_6$ (electrolyte no. 3), where $R_1°$ and R_1^s were observed to range between 350 and 2200 Ω, and T_+ of about 0.01 was obtained.

The preceding data appear to indicate that there is a correlation between the highly resistive passivation layers and the very small cationic transference numbers obtained. As mentioned earlier, these electrolytes have high ionic conductivities which translates into a bulk resistance, R_b, of about 3 Ω. When a dc bias of 7.5 mV is applied across the cell, the potential drop across the electrolyte is calculated to be $I°R_b = 0.08$ mV, while that across the passivation layer is $I°R_1° = 7.4$ mV. Hence, the applied potential is used to transport ions primarily in the resistive passivation layer rather than in the electrolyte. The transference numbers thus obtained will not be an accurate representation of the transport properties of the electrolytes.

To compensate for the large potential loss across the passivation layers, the applied dc bias was increased to between 50 and 100 mV. The electrolyte thickness was also increased to about 130 μm to increase the relative resistance of the electrolyte compared to that of the passivation layers.

For electrolyte no. 2 (expt 2(e) in Table 6) subjected to a 48 mV dc bias, the initial and final impedances of the cell gave $R_1° = 116.6$ Ω and $R_1^s = 103.6$ Ω, showing an overall decrease in the resistance of the passivation layer during polarization. The bulk resistance of the electrolyte was 19.2 Ω, and the potential drop across the electrolyte was calculated to be $I°R_b = 6.8$ mV, while that across the passivation layer was $I°R_1° = 41$ mV. The cationic transference number calculated from eq 6 was 0.34.

Table 6. Summary of Transference Number Measurements Obtained with dc Biases between 48 and 78 mV

electrolyte no.	expt	$R_1°$ (Ω)	R_1^s (Ω)	$I°$ ($\times 10^{-5}$ A)	I^s ($\times 10^{-5}$ A)	V (mV)	T_+
2	e	116.6	103.6	3.52	2.99	48	0.34
	f	145.7	141.4	2.70	2.03	48	0.34
	g	202.3	272.2	2.15	1.33	48	0.24
3	d	85.9	358	7.9	1.9	78	0.24
	e	114.9	359.7	6.2	2.0	78	0.36
	f	81.3	310.1	5.0	1.3	48	0.22
	g	147.3	723.0	3.4	0.71	58	0.23

A dc bias of 78 mV was applied across a cell containing electrolyte no. 3 (Table 6, expt 3(d)). A significantly higher current ($I_0 = 7.9 \times 10^{-4}$ A) was measured as compared to that observed at the smaller dc bias of 7.5 mV ($I_0 = 2.04 \times 10^{-5}$ A, see Table 5). From the initial and final impedances of the cell, $R_1° = 85.9$ Ω and $R_1^s = 358$ Ω were calculated. The bulk resistance of the electrolyte was 12.3 Ω, and the potential drop across the electrolyte was calculated to be 9.7 mV. The cationic transference number was calculated to be 0.24 from eq 6.

Several transference number measurements were carried out for electrolyte nos. 2 and 3 with dc biases ranging between 48 and 78 mV, and the results are summarized in Table 6. With the exception of one measurement for each electrolyte, 2(g) and 3(e), the T_+ obtained were fairly consistent. A marked improvement was observed for electrolyte no. 3, where a T_+ of about 0.2 was obtained at several different applied potentials, as compared to 0.01 obtained earlier. It is clear from the preceding discussion that the transference number measurements have large uncertainties, but the values obtained are reasonably accurate to indicate the nature of principal current carrying species in these electrolytes.

It can be concluded that overall PAN-based electrolyte containing $LiAsF_6$, $LiN(CF_3SO_2)_2$, and $LiPF_6$ have relatively low cationic transference numbers of 0.13, 0.34, and 0.24, respectively. This indicates that anionic species are the key contributors to the total ionic conductivity in this system. This behavior of these electrolytes is reminiscent of conventional organic liquid electrolytes.

Mechanical Strength. The mechanical strength of PAN-based electrolyte (100 μm) was measured and compared to that of polypropylene (25 μm thick Celgard membrane) and polyethylene (75 μm thick) films. The stress/strain curves are reported in Figure 7. Three important properties can be characterized from a stress−strain curve.

(i) Elastic modulus (EM): measure of resistance to deformation obtained from the slope of the stress/strain curve in the elastic region.

(ii) Ultimate tensile strength (UTS): stress required to rupture the sample.

(iii) Ultimate elongation (UE): extent of elongation at the point of rupture.

The commercial polymers have high tensile strengths and low elongation-at-break (strain) values. The PAN-based electrolyte has the opposite properties; a relatively high strain value and a low tensile strength. Typically, polymers with a high degree of crystallinity or cross-linking or rigid chains (characterized by high T_g) exhibit high strength and low extendability. Conversely, high

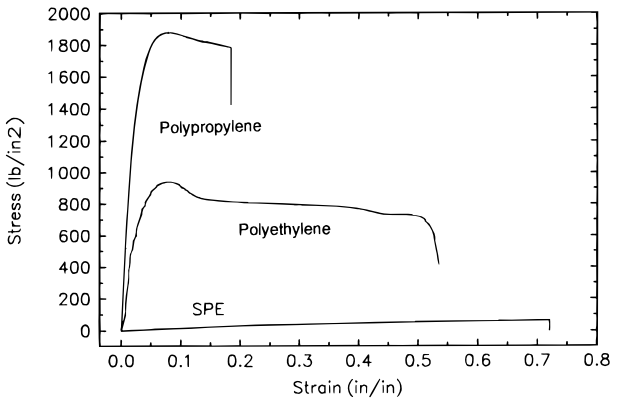

Figure 7. Stress−strain curves of Celgard polypropylene, low-density polyethylene, and SPE membranes.

Table 7. Conductivities of Some PAN-Based Electrolytes with and without Interpenetrating Networks

electrolyte no.	PAN (w/o)	EC (w/o)	PC (w/o)	$LiPF_6$ (w/o)	other (w/o)	RT conductivity (10^{-3} Ω^{-1} cm^{-1})
SPE1	13.0	59.2	14.8	13.0		3.78
A	12.5	56.6	14.2	12.5	(VS) 4.2	2.00
B	12.5	56.6	14.2	12.5	(EGD) 4.2	1.43

extendability and low tensile strength are usually characteristics of polymers with low crystallinity and cross-linking and low T_g. The PAN-based electrolytes belong to the latter group. It should be noted that the tensile strength of PAN-based electrolytes is adequate for their use as separators in batteries (see below) and their relatively high ultimate elongation (strain) is indicative of a pliable material which would lend itself to form "soft or conforming" interfaces with electrodes.

The mechanical properties of the electrolyte films could be modified with the use of interpenetrating networks (IPN), formed from in situ thermal polymerization of additives such as vinyl sulfone (VS) and ethylene glycol dimethacrylate (EGD). The former forms poly(vinyl sulfone) (PVS) and the latter yields poly(ethylene glycol dimethacrylate) (PEGD) upon polymerization.

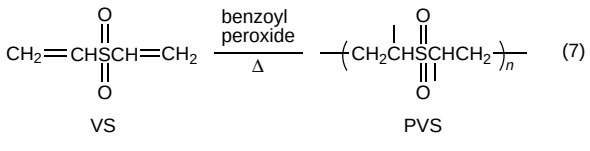

(7)

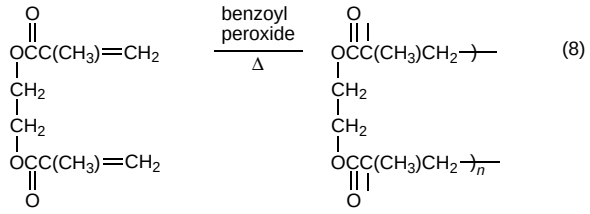

(8)

The electrolyte containing the poly(vinyl sulfone) IPN showed an increase in the UE from 70 to 190%, although its tensile strength did not change much from that of the baseline material (55 versus 60 lb/in^2). The electrolyte cross-linked with EGD, on the other hand, had a higher tensile strength of 140 lb/in^2 with little change in the UE. The conductivities of the modified electrolytes were slightly lower (Table 7) but quite adequate for the fabrication of room temperature polymer electrolyte batteries. The improved strength of the EGD-modified electrolyte may be beneficial in connection with its handling and processing.

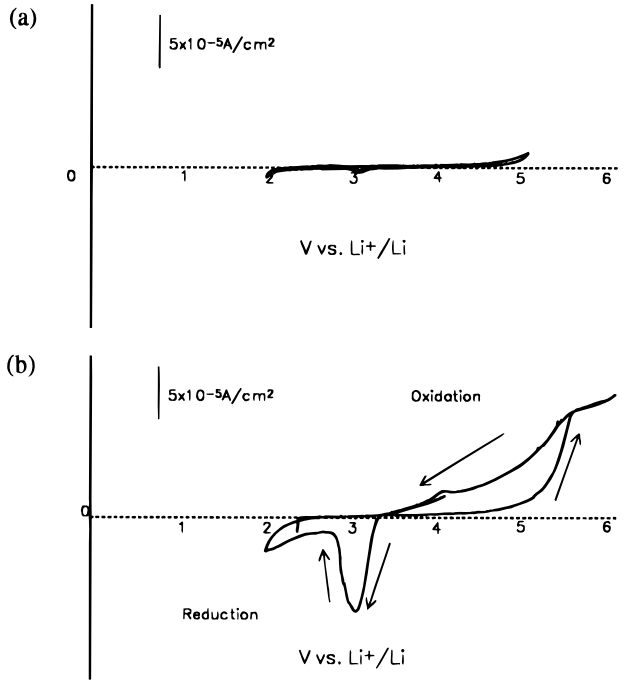

Figure 8. Cyclic voltammograms of PAN-based electrolyte containing $LiN(CF_3SO_2)_2$ on a Pt substrate. The EC:PC ratio in the electrolyte is 4:1 by weight. Sweep rate = 1 mV/s: (a) between 2 and 5 V; (b) between 2 and 6 V.

Oxidative Stabilities of PAN-Based Electrolytes. The electrochemical stability of an electrolyte is determined by the redox properties of the polymer host, the plasticizer solvents, and the Li salt it contains. When experimentally determining an electrolyte's oxidative stability, the corrosion of the metal electrode on which the electrochemical reaction is performed must be distinguished from the oxidation reactions of the electrolyte. The electrode corrosion will be influenced by the Li salt since the anion of the salt will influence the solubility of the corrosion products, which in turn will determine the kinetics of the corrosion reaction. Thus, a knowledge of the corrosion behavior of metals as a function of the nature of the Li salt in the electrolyte is extremely important in fully describing the oxidative stability of the electrolyte and in determining the usefulness of the metals as current collectors in batteries containing the electrolyte.

The oxidative stabilities of the electrolytes were determined from slow sweep cyclic voltammetry by potential cycling the working electrode between 2 and 4.2 V at a scan rate of 1 mV/s. The oxidation potential was taken as the potential at which a sharp increase in the current from the baseline (i.e., >20 μA/cm^2) was observed.

Pt Electrode. Platinum was used as a substrate in an attempt to study the inherent stability of the various electrolytes toward oxidation. The voltammograms in Figure 8 are representative of the behavior of PAN-based electrolytes on this electrode. Oxidation of the electrolytes occurs at potentials beyond 5 V. Once the oxidation begins, however, the current persists in the reverse scan down to about 3.5 V and a corresponding reduction peak appears at around 3 V. Because of their similar electrochemical behavior, it can be concluded

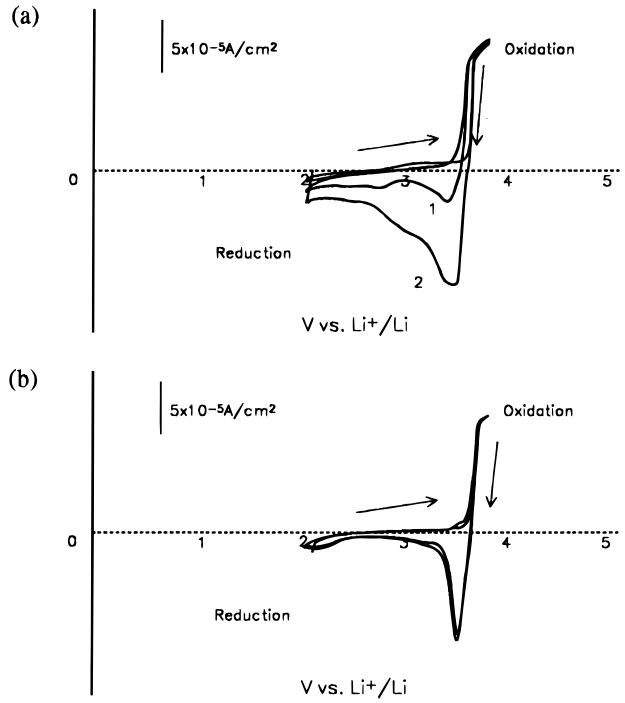

Figure 9. Cyclic voltammograms of electrolytes containing (a) $LiN(CF_3SO_2)_2$ and (b) $LiPF_6$ on Cu substrate. EC:PC ratio in the electrolyte is 4:1 by weight. Sweep rate = 1 mV/s.

that electrolytes containing $LiCF_3SO_3$, $LiN(CF_3SO_2)_2$, $LiPF_6$, and $LiAsF_6$ are all inherently stable up to about 5 V. The inherent oxidation stability of the electrolyte, however, can be observed only with a corrosion-free electrode such as Pt. On the other electrodes, the electrolyte's stability limit is masked by electrode corrosion.

Cu Electrode. Copper is more easily oxidized than Ni and Al. The oxidation process at about 3.5 V (Figure 9) is reversible and probably corresponds to the reaction

$$Cu \rightleftarrows Cu^{2+} + 2e^- \qquad (9)$$

involving the oxidation of Cu to Cu^{2+}. There is very little influence of anions on this process, nor is there any evidence of Cu passivity from the salts. It appears that the probable corrosion products, $Cu(PF_6)_2$ and $Cu[N(SO_2CF_3)_2]_2$, are soluble in the PAN-based electrolytes allowing the corrosion reaction to continue unabated. A corrosion potential of 3.5 V is consistent with the oxidation of Cu to Cu^{2+}, as previously found in $SOCl_2$[9] and organic electrolytes.[10] The oxidation of Cu to Cu^+ is believed to occur at about 2 V.

Ni Electrode. Figure 10a shows the voltammograms of electrolyte no. 3, containing $LiN(CF_3SO_2)_2$, on a Ni electrode. An oxidation reaction is observed starting at around 3.5 V with the current increasing to 130 μA/cm^2 at 4.2 V. To see the effect of the relative amounts of EC and PC on oxidation stability, voltammetric measurements were carried out on electrolyte no. 4 (containing a 4:1 by weight of EC:PC) and no. 5 (containing only EC). The data presented in Figures 10b,c show that regardless of the relative amounts of EC and PC in PAN−EC−PC−$LiN(CF_3SO_2)_2$, oxidation reactions on Ni start at about 3.5 V.

An oxidation reaction starting at around 3.5 V was also observed in electrolyte no. 9 containing $LiPF_6$. Again, different amounts of EC and PC had no influence

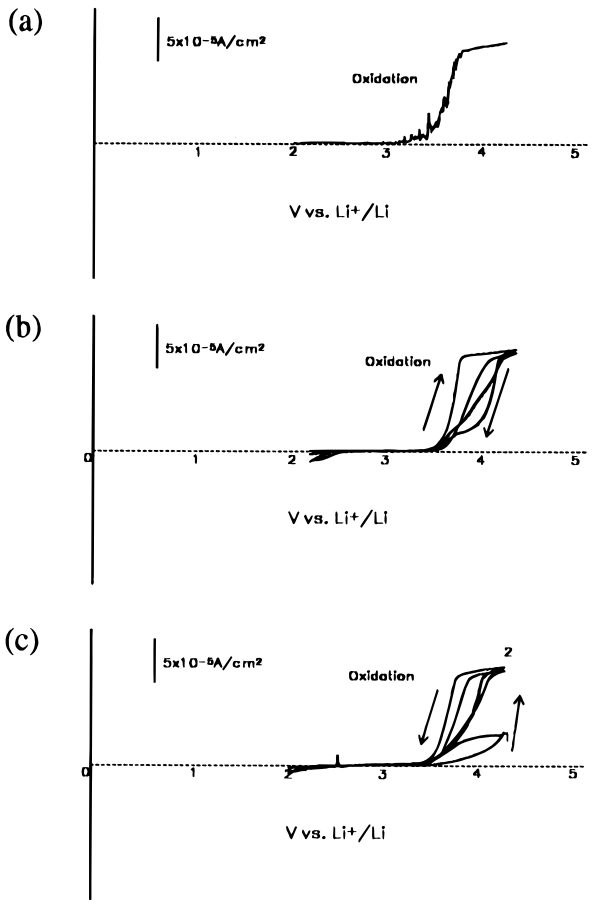

Figure 10. Cyclic voltammograms of electrolytes containing $LiN(CF_3SO_2)_2$ with EC and PC at the ratios of (a) 1:1, (b) 4:1, and (c) 1:0 by weight. The electrode is nickel. Sweep rate = 1 mV/s.

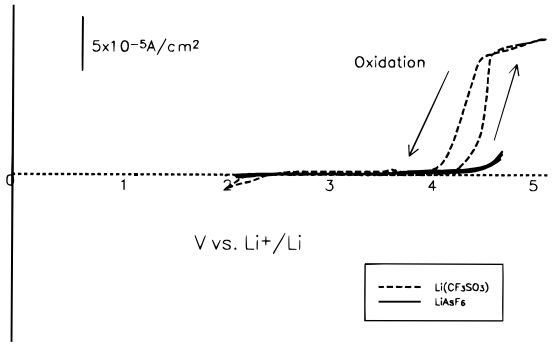

Figure 11. Cyclic voltammograms of electrolytes containing $Li(CF_3SO_3)$ (dotted line) and $LiAsF_6$ on a Ni electrode. The EC:PC ratio in the electrolyte is 1:1 by weight. Sweep rate = 1 mV/s.

on the onset potential of oxidation; in all cases, oxidation started at around 3.5 V with currents increasing to 100−145 μA/cm^2 by 4.2 V. The behavior of electrolytes containing $LiCF_3SO_3$ was similar to those based on $LiN(SO_2CF_3)_2$.

In contrast to the electrolytes containing $LiN(CF_3SO_2)_2$, $LiCF_3SO_3$, and $LiPF_6$, those containing $LiAsF_6$ (electrolyte nos. 6 and 8) appeared to be stable up to about 4.4 V on Ni independent of the relative amounts of the two solvents (see Figure 11).

The corrosion reactions of the Ni electrode can be explained in the same way as that for Cu involving the formation of soluble corrosion products. It appears that Ni is oxidized to Ni^{2+} at about 3.5 V, probably to form

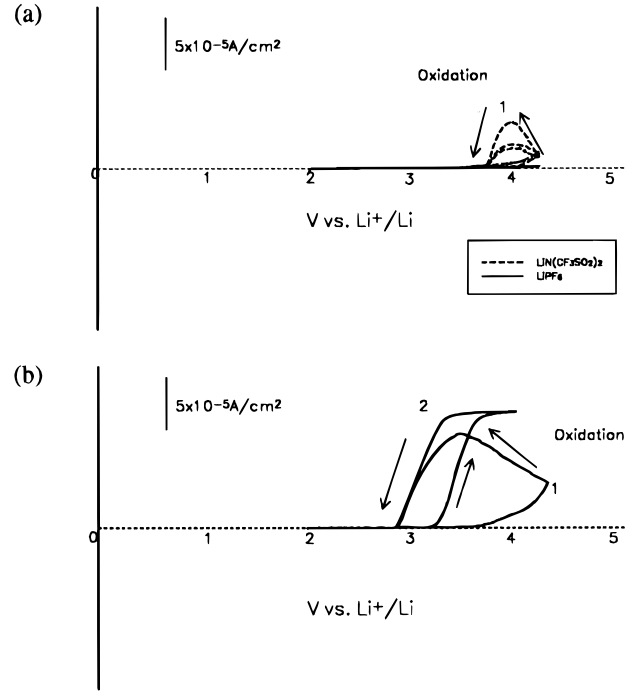

Figure 12. Cyclic voltammograms of electrolytes containing (a) $LiN(CF_3SO_2)_2$ (electrolyte no. 3) (dotted line) and $LiPF_6$ (electrolyte no. 9) (solid line) on Al substrate, (b) $LiCF_3SO_3$ (electrolyte no. 1) on Al. Sweep rate = 1 mV/s.

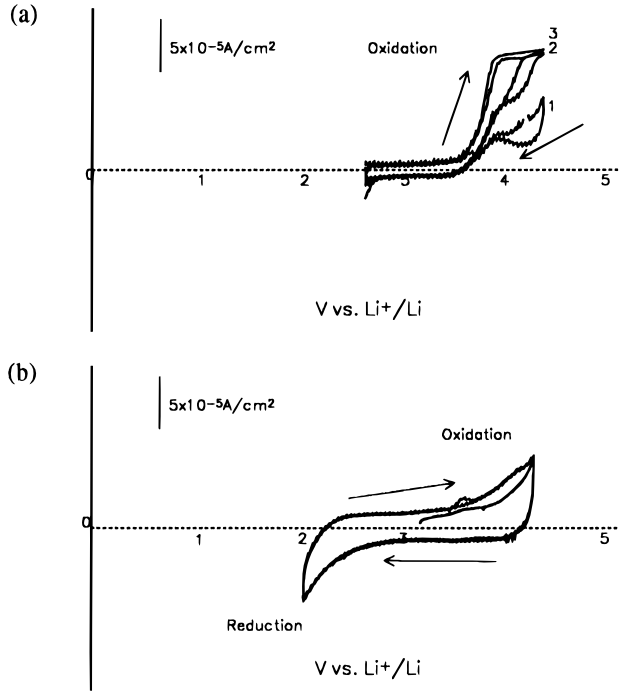

Figure 13. Cyclic voltammograms of electrolyte no. 4 containing $LiN(CF_3SO_2)_2$ on carbon substrate with (a) Al and (b) SS as current collectors. The EC:PC ratio in the electrolyte is 4:1 by weight. Sweep rate = 1 mV/s.

$Ni(PF_6)_2$, $Ni[N(SO_2CF_3)_2]_2$, and $Ni(SO_3CF_3)_2$ in electrolytes containing $LiPF_6$, $LiN(SO_2CF_3)_2$, and $LiSO_3CF_3$, respectively. These nickel salts appear not to passivate Ni, again probably due to their solubility in PAN-based electrolytes. The exceptionally high oxidation potential of Ni in $LiAsF_6$-based electrolytes (i.e., ~4.4 V) may be explained by the passitivity afforded to it by the poorly soluble $Ni(AsF_6)_2$. An alternative explanation is the formation of a NiF_2 film.

Al Electrode. Figure 12 gives a comparison of the oxidation stabilities of electrolytes no. 3 and 9, containing $LiN(SO_3CF_3)_2$ and $LiPF_6$, respectively. The electrolyte containing $LiN(CF_3SO_2)_2$ undergoes oxidation below 4 V while that containing $LiPF_6$ appears to be oxidatively stable up to 4.2 V. Different ratios of EC and PC in the electrolytes had no effect on the oxidation potentials. The observation that the electrolyte containing $LiN(SO_2CF_3)_2$ showed significant oxidation currents below 4 V only after it was cycled first to 4.2 V indicates that the most probable reaction is Al corrosion. It appears that the aluminum oxide passivation layer which protects Al against corrosion breaks down at potentials near 4.2 V.

Electrolytes containing $LiCF_3SO_3$ behaved in a manner similar to those containing $LiN(SO_3CF_3)_2$, whereas the behavior of those containing $LiAsF_6$ was reminiscent of their $LiPF_6$ counterparts (Figure 12). Again, the loss of passivity of Al following the destruction of the aluminum oxide passivation layer in the electrolytes containing $LiN(SO_2CF_3)_2$ and $LiCF_3SO_3$, can be attributed to the solubility of the corrosion products, $Al(CF_3SO_3)_3$ and $Al[N(SO_2CF_3)_2]_3$, in the electrolyte. On the contrary, Al has better passivity in electrolytes containing $LiPF_6$ and $LiAsF_6$.

SS Electrode. Stainless steel was used as a substrate in combination with electrolytes containing $LiN(CF_3SO_2)_2$ (electrolyte no. 4), $LiPF_6$ (electrolyte no. 10) and $LiAsF_6$ (electrolyte no. 6). All three electrolytes showed good oxidative stability within the potential range of 2−4.2 V.

Carbon Electrode. Since the electrodes used in a battery often are made up of high surface area carbon, voltammetric experiments were also carried out on carbon electrodes fabricated from carbon black (i.e., Chevron acetylene black) with a surface area of ~40 cm^2/g. Al and SS were used as the current collectors for the carbon electrodes.

Figure 13 shows the data for electrolyte no. 4, containing $LiN(CF_3SO_2)_2$ and a 4:1 by weight of EC/PC. The significantly higher charging (baseline) current observed for carbon than the metal electrodes reflects the large surface area of the carbon. The electrolyte undergoes oxidation at around 3.5 V when Al is used as the current collector, but is stable up to 4.2 V when SS is used. These results correlate with the voltammetric results on bare Al and SS electrodes, discussed earlier. The observation from electrolyte no. 4 that electrolyte stability on carbon depends on the nature of the metal current collector used was confirmed from experiments with electrolytes containing $LiPF_6$ (electrolyte no. 10) and $LiAsF_6$ (electrolyte no. 8). These electrolytes were resistant to oxidation on carbon up to 4.2 V with both Al and SS current collectors.

Metal Electrode Corrosion versus Electrolyte Oxidation. The electrochemical data indicate that PAN-based electrolytes containing $LiN(SO_2CF_3)_2$, $LiAsF_6$, $LiPF_6$, and $LiSO_3CF_3$ are all inherently stable up to about 5 V. The Li salt plays a key role on the "apparent" electrochemical oxidative stabilities on Ni, Al, and Cu. For example, electrolytes containing $LiPF_6$ and $LiAsF_6$ are oxidatively more stable on Al than those containing $LiN(CF_3SO_2)_2$ and $LiCF_3SO_3$. On Ni, stability beyond 4 V is found only when the salt is $LiAsF_6$.

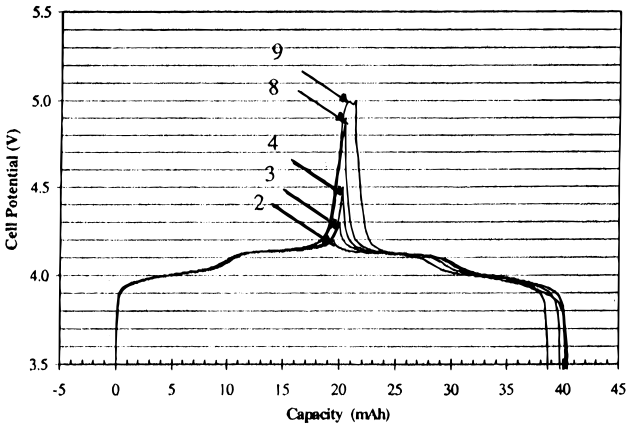

Figure 14. Representative charge and discharge curves of a Li/SPE/$LiMn_2O_4$ cell with charge limits ranging between 4.2 and 5 V. The cycle numbers are indicated on the curves. The SPE was PAN−EC/PC−$LiAsF_6$ and $I_c = I_d = 0.1$ mA/cm^2.

These differences are understood from considerations of the corrosion reactions of the metal electrodes.

Cu is reversibly oxidized in the presence of all of the Li salts studied. The corrosion reactions of Al and Ni are anion dependent. Some of the anions afford passivity to these metals, apparently due to the low solubility of the corrosion products formed. Ni is afforded little passivity by $LiPF_6$, $LiN(SO_2CF_3)_2$, and $LiSO_3CF_3$ while its oxidative stability is extended to ~4.2 V by $LiAsF_6$. Aluminum is stable up to 4.2 V in the presence of $LiPF_6$ and $LiAsF_6$, while the fluorinated organic anion-containing salts corrodes these metals at potentials below 4.2 V.

Li/SPE/$LiMn_2O_4$ Cells. The oxidative stability of PAN-based electrolyte was further confirmed by incorporating the polymer electrolyte as a separator in Li/$LiMn_2O_4$ cells. Figure 14 shows the galvanostatic cycling curves of a Li/$LiMn_2O_4$ cell containing PAN−EC/PC−$LiAsF_6$ as the separator. The charge voltage limit was increased from 4.2 and 5 V vs Li^+/Li at various stages of the cycling experiment. The data summarized in Table 8 indicate that the cell can be charged up to 4.9 V vs Li^+/Li without any electrolyte decomposition and capacity irreversibility. The long-term cycling data for a Li/$LiMn_2O_4$ cell containing the same electrolyte as the separator and cycled between 3 and 4.2 V are displayed in Figure 15. The cell underwent more than 100 cycles with a discharge capacity corresponding to an average utilization of 0.61 Li/mol of $LiMn_2O_4$, and a capacity fade rate of 0.2% per cycle. These data confirm the oxidative stability of PAN-based electrolytes, and their usefulness as a separator in all-solid-state rechargeable batteries.

Table 8. Charge Limit and Charge and Discharge Capacities of a Li/SPE/$LiMn_2O_4$ Cell

cycle no.	charge limit (V)	charge capacity (mAh)	discharge capacity (mAh)
1	4.2	20.2	19.7
2	4.2	19.5	19.3
3	4.3	20.0	19.9
4	4.5	20.3	20.1
5	4.5	20.1	19.6
6	4.7	20.4	17.8
7	4.7	20.4	20.0
8	4.9	20.2	20.2
9	5.0	21.3	19.4
10	5.0	19.3	19.1
11	4.2	16.3	17.0
12	4.2	17.2	17.5
13	4.3	18.6	18.6
14	4.3	18.5	18.5
15	4.3	18.4	18.4
16	4.3	18.3	18.3
17	5.0	20.0	19.5

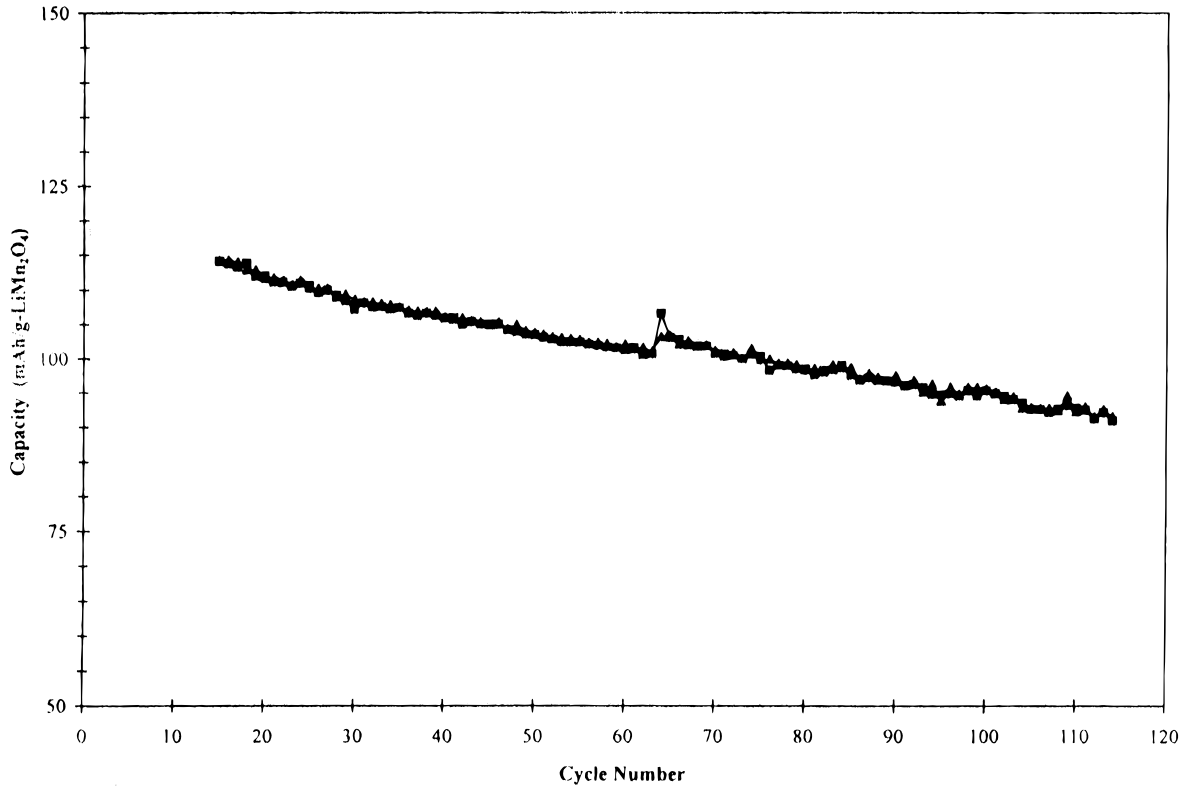

Figure 15. Long-term galvanostatic cycling data of a Li/SPE/$LiMn_2O_4$ cell cycled between 3 and 4.2 V at $I_c = 0.1$ mA/cm^2 and $I_d = 0.7$ mA/cm^2. The SPE was PAN−EC/PC−$LiAsF_6$.

Conclusions

Polyacrylonitrile-based electrolytes have been prepared with conductivities as high as $4.5 \times 10^{-3}\ \Omega^{-1}\ cm^{-1}$ at 30 °C. The cationic transference numbers ranging between 0.13 and 0.34 indicate that the conductivity is dominated by anionic mobilities. The tensile strength of the electrolytes was observed to increase from 60 to 140 lb/in.^{2} upon incorporation of an interpenetrating network of poly(ethylene glycol dimethacrylate). Cyclic voltammetry on Pt showed that these electrolytes have an inherent oxidative stability window extending up to about 5 V versus Li^+/Li. Lower oxidation potentials were observed on Al, Ni, and Cu electrodes because of metal corrosion reactions. The nature of the Li salt in the electrolyte influenced the potential for the onset of the corrosion reaction. Electrolytes containing $LiPF_6$ and $LiAsF_6$ exhibited good oxidative stabilities on Al, SS, and carbon (Table 9). This was confirmed in a Li/SPE/$LiMn_2O_4$ cell, which showed good rechargeability without any electrolyte decomposition even when it was charged to 4.9 V vs Li/Li^+. PAN-based electrolytes are excellent candidates for use as separators in Li and Li-ion batteries containing the high voltage cathodes $LiMn_2O_4$, $LiNiO_2$, and $LiCoO_2$. Aluminum seems to be a good choice as a cathode current collector, which has the added advantage of being very light.

Table 9. Influence of Li Salts on the Oxidation Stability Limits (volts versus Li^+/Li) of PAN-Based Electrolytes on Various Electrodes

Li salt	Ni	Al	Cu	SS	C/SS	C/Al	Pt
$LiN(CF_3SO_2)_2$	3.5	3.7	3.5	4.2	4.2	3.7	5
$LiPF_6$	3.5	4.2	3.5	4.2	4.2	4.2	5
$LiAsF_6$	4.4	4.2	*a*	4.2	4.2	4.2	5
$Li(CF_3SO_3)$	4.1	3.5	*a*	*a*	4.2	*a*	5

[a] Not determined.

Acknowledgment. Financial support for this work was provided by the Department of Energy, Contract No. DEF02-91-CE50336.

CM9604120